Organic & Biomolecular Chemistry

ROYAL SOCIETY OF CHEMISTRY

PAPER

View Article Online
View Journal | View Issue

Cite this: *Org. Biomol. Chem.*, 2024, **22**, 4123

Structure and isomerization behavior relationships of new push–pull azo-pyrrole photoswitches†

D. Gallardo-Rosas,[a] J. M. Guevara-Vela,[b] T. Rocha-Rinza,[c] R. A. Toscano,[c] J. G. López-Cortés[c] and M. C. Ortega-Alfaro*[a]

Received 14th March 2024,
Accepted 30th April 2024

DOI: 10.1039/d4ob00417e

rsc.li/obc

A family of stilbenyl-azopyrroles compounds **2a–d** and **3a–d** was efficiently obtained *via* a Mizoroki–Heck C–C-type coupling reaction between 2-(4′-iodophenyl-azo)-*N*-methyl pyrrole (**1a**) and different vinyl precursors. The influence of the π-conjugated backbone and the effect of the pyrrole moiety were correlated with their optical properties. Studies *via* UV-Visible spectrophotometry revealed that the inclusion of EWG or EDG favors a red-shift of the main absorption band in these azo compounds compared with their non-substituted analogues. Furthermore, there is a clear influence between the half-life of the *Z* isomer formed by irradiation with white light and the push–pull behavior of the molecules. In several cases, the stilbenyl-azopyrroles led to the formation of J-type aggregates in binary MeOH : H_2O solvents, which are of interest for water compatible applications.

Introduction

The development of strategies to control molecular motion is a central concept in a wide variety of areas, such as molecular machines,[1] molecular recognition,[2] self-assembly,[3] and catalysis.[4] Particularly, heteroaryl azo-compounds including nitrogen-based heterocycles such as pyridine,[5] pyrrole,[6] pyrazole,[7] imidazole,[8] benzimidazole,[9] thiazole,[10] benzothiazole,[11] and indole[12] are emerging as a new class of highly efficient and versatile molecular photoswitches. These compounds are of great interest due to their ability to carry out reversible and selective photoinduced transformations by using a defined wavelength. Additionally, these molecules exhibit nearly quantitative *E*–*Z* isomerization with tunable thermal lifetimes.[8,9–12]

In this context, azo compounds containing a push–pull system incorporated into their structure display interesting nonlinear optic and solvatochromic properties, which can be used in the design of opto-electronic materials.[12–15] The molecular polarization of push–pull systems has key implications for the optical response at the molecular level. The optimization of π-conjugated linkers, electron-donor, and electron-acceptor groups are relevant design variables to consider in this regard.[16] Recently, we demonstrated that push–pull properties are efficiently modulated by using a functionalized biphenyl moiety as a π-linker, in combination with a pyrrole ring on each side of the N=N azo group. This molecular architecture provokes a red-shift to the visible region of the π/π* band of the azo-group, an increasing in its molar absorption coefficient,[13] and a reversible photoisomerization upon irradiation using a white LED. This strategic design has been extended to some examples of push–pull azo-compounds, including a stilbenyl fragment that can be photoisomerized upon two-photon excitations.[14,16]

As an ongoing program for the synthesis and photophysical studies of π-extended azo-heteroarene compounds, we report herein a general method for the obtainment of a family of push–pull azopyrroles bearing several stilbenyl motifs directly bonded to the N=N azo group. The key synthetic strategy is based on the Mizoroki–Heck coupling reaction catalyzed by a robust palladium source as catalyst, with different vinyl precursors as coupling partners (Scheme 1).

Results and discussion

The synthesis of this family of π-extended azopyrrole compounds **2a–d** began with the preparation of **1**, following a well-established azo-coupling reaction between *N*-methylpyrrole and 4-iodoaniline.[14,15] Then, we reacted precursor **1** with diverse *p*-substituted styrenes in presence of [Pd/(*N*,*N*)-pyrrole ligand].

[a]*Instituto de Ciencias Nucleares, UNAM, Circuito Exterior, Ciudad Universitaria, Coyoacán C.P. 04510, Ciudad de México, Mexico.*
E-mail: carmen.ortega@nucleares.unam.mx
[b]*Departamento de Química Física Aplicada, Universidad Autónoma de Madrid, 28049 Madrid, Spain*
[c]*Instituto de Química UNAM, Circuito Exterior, Ciudad Universitaria, Coyoacán C.P. 04510, Cuidad de México, Mexico*

† Electronic supplementary information (ESI) available: Experimental procedures and characterization data of all compounds. CCDC 2189449 (**3b**). For ESI and crystallographic data in CIF or other electronic format see DOI: https://doi.org/10.1039/d4ob00417e

Scheme 1 Retrosynthetic approach to obtain push–pull stilbenyl azo-pyrroles.

This palladium complex demonstrated to be a robust and efficient catalytic precursor to promote the Mizoroki–Heck coupling using demandant substrates as ethylene and other azo-pyrrole compounds (Table 1, entries 5–7).[18] Using this methodology, we obtained the new π-extended azo-pyrroles dyes **2a–d** as orange or red solids in good to moderated yields. In the case of **2c** and **2d**, we observed the formation of lateral products. The molecular identities of these compounds agree with the spectroscopical data obtained by NMR, IR and MS analyses. For instance, the ^{1}H NMR spectrum of **2a** shows a doublet at 7.76 ppm (J = 9.0 Hz) assigned to 2 hydrogens of a phenyl group adjacent to a C=C double bond. Between 7.55 and 7.52 ppm, we observe a multiple signal (6H) assigned to the rest of protons of 1,4-disustituted phenyl rings. Likewise, an AB system (J = 15 Hz) at 7.16 and 7.09 ppm confirm the presence of the double bond with an *E* geometry. Additionally, three multiplets at 6.88, 6.66 and 6.24 ppm correspond to hydrogens in position 5, 3 and 4 (respectively) on the pyrrole ring. A singlet at 3.9 ppm is assigned to a methyl group. In the ^{13}C NMR spectrum, we can find the corresponding signals for the double bond of the stilbene moiety at 130.6 and 127.7 ppm that confirms the C–C coupling between 1 and 4-trifluoro-methyl styrene. Similar spectroscopic data are obtained for this series of azo-compounds **2a–d**.

We successfully extended this methodology to other vinyl heteroarenes, thereby obtaining the π-extended azopyrroles **3a–d** in good yields (Table 2). In a similar fashion to azo-dyes **2a–d**, these compounds were obtained as orange and red solids in yields ranging from 53 to 82%. Again, we observed the formation of some vinyl oligomers as side products derived of lateral oligomerization of vinyl reagents, mainly for the case of the synthesis of **3c**. The molecular identities of these compounds were confirmed by conventional spectroscopic techniques. For instance, the ^{1}H NMR spectrum of **3b** displays a set of doublets at 8.59 and 7.38 ppm (J = 9 Hz) assigned to the 4-pyridin fragment. At 7.83 and 7.62 ppm, two set of signals are observed for the protons of the phenyl ring adjacent to the azo group. Likewise, an AB system (J = 15 Hz) at 7.34 and 7.07 ppm confirms the double bond formed after the coupling reaction. The protons of the pyrrole ring appear at 6.96, 6.74 and 6.32 ppm. The methyl group bonded to the nitrogen atom of the pyrrole group is identified as a singlet at 3.97 ppm.

Single crystals of **3b** allow to confirm its structure by X-ray monocrystal diffraction (Fig. 1). The azo group exhibits an *E* geometry and the bond distance between the N atoms in the azo group [N(2) and N(3)] is longer than that reported for azobenzene [1.273(3) Å] but shorter than that observed in other azopyrrole dyes.[14,15] This behavior reveals that although the pyridine group is a π-deficient group, its electron withdrawing effect is not comparable to that of $-CF_3$ or $-NO_2$ groups. Hence, the molecule is less coplanar displaying a torsion angle of approximately 10° between the plane formed by C12–C13–C6 and C13–C14–C15.

In order to modify the optical properties of **3a–c** and to increase the electron acceptor character of the heterocyclic moieties included in these compounds, we carried out an alkylation reaction to obtain a new series of push–pull azo

Table 1 Heck–Mizoroki cross-coupling of **1a** and different styrenes[a]

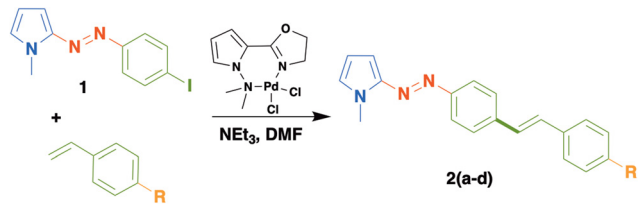

Entry	Compound	R	Time (h)	Yield[b] (%)
1	**2a**	CF_3	2	71
2	**2b**	CN	3	73
3	**2c**	Br	1	58
4	**2d**	OMe	1	57
5	**2e**	H	1	90[15]
6	**2f**	NO_2	1	82[15]
7	**2g**	NMe_2	2	78[15]

[a] All reactions were performed with 1 mmol of **1a**, 1.2 mmol of the corresponding styrene, DMF (5 mL) and 1.2 mmol of NEt_3, 0.1% mol of [Pd] at 160 °C. [b] Isolated yield after SiO_2 column chromatography.

Table 2 Heck–Mizoroki cross-coupling of **1a** and different vinyl precursors[a]

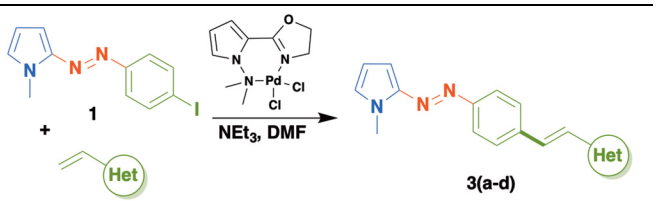

Entry	Compound	Het	Time (h)	Yield[b] (%)
1	**3a**	Fc	2	69
2	**3b**	4-Pyridinyl	1	73
3	**3c**	3-Pyridinyl	1	53
4	**3d**	4-Quinolinyl	2	82

[a] All reactions were performed with 1 mmol of **1a**, 1.2 mmol of the corresponding vinyl precursor, DMF (5 mL) and 1.2 mmol of NEt_3, 0.1% mol of [Pd] at 160 °C. [b] Isolated yield after SiO_2 column chromatography.

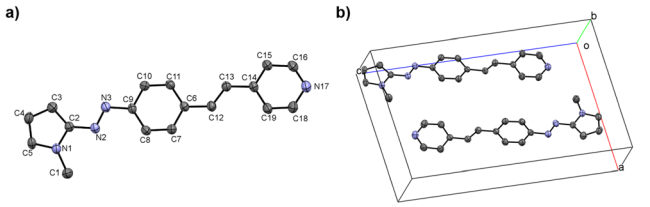

Fig. 1 ORTEP representation of **3b**. Ellipsoids are shown at 30% of probability. N(1)–C(1) 1.452(4), N(1)–C(2) 1.378(3), N(1)–C(5) 1.350(4), N(2)–N(3) 1.273(3), N(2)–C(2) 1.385(3), N(3)–C(9) 1.419(3), C(2)–C(3) 1.375(4), C(3)–C(4) 1.383(4), C(4)–C(5) 1.365(4), C(6)–C(12) 1.461(3), C(12)–C(13) 1.321(3), C(13)–C(14) 1.467(4), C(14)–C(15) 1.380(3), C(14)–C(19) 1.391(3), C(15)–C(16) 1.381(4), C(16)–N(17) 1.322(4), N(17)–C(18) 1.323(4), C(18)–C(19) 1.367(4), (b) crystal lattice of **3b**.

dyes **4b–d** as solid salts, in excellent yields (Table 3). The formation of these new azo-compounds was confirmed by conventional spectroscopic techniques. The ^{1}H-NMR spectrum of **4b** reveals distinct changes in the chemical shifts of protons of the 4-pyridinum fragment which are shifted to higher frequencies (8.88 and 8.35 ppm) in comparison to those of compound **3b**. Likewise, the protons of the double bond are shown as an AB system registered at 8.08 and 6.60 ppm (J = 15 Hz). The protons of 1,4-disubstituted phenyl rings appear as a multiplet at 7.88 ppm and the protons of the pyrrole ring are recorded at 7.38, 6.67 and 6.35 ppm. Two singlets at 4.27 and 3.96 ppm are assigned to the methyl groups included in the pyridinium fragment and in the pyrrole ring, respectively.

UV-Visible studies of stilbenylazopyrrole dyes

The UV/vis spectra of π-extended biphenyl-azopyrroles **2a–d** and **3a–d** acquired in MeOH are shown in Fig. 2. In general, we observe non-significant changes in the position of λ_{max} by virtue of the substituent. These compounds display a π–π* transition near 420 nm and an n–π* transition around 440 nm

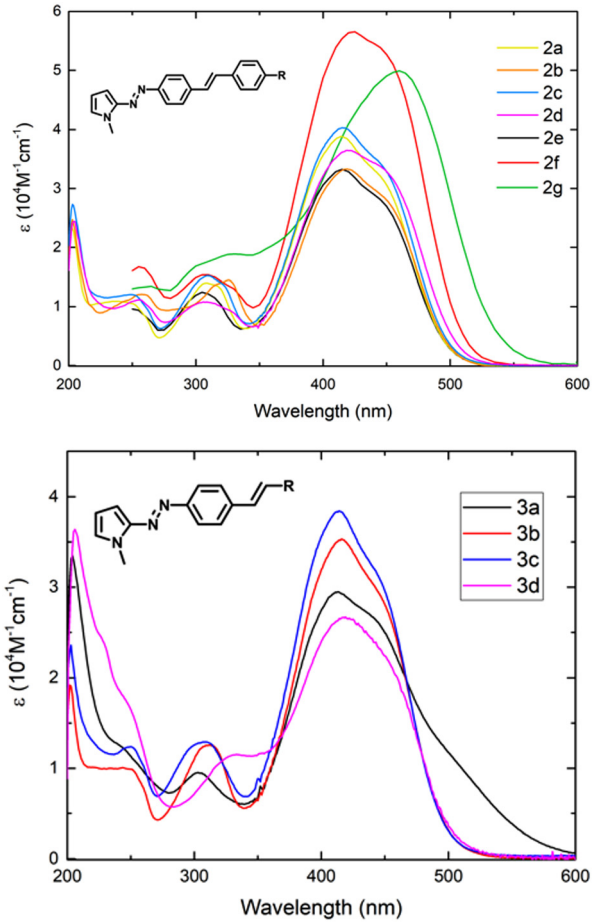

Fig. 2 UV-Visible spectra of **2a–g** (top) and **3a–d** (dawn) acquired in MeOH.

as a shoulder on the π–π* transition band. When the phenyl group in azobenzene is replaced by a π-electron rich system like *N*-methylpyrole, we noted an important bathochromic shift of the main absorption band from 320 nm[19] to 385 nm.[11,15] We recently informed that this absorption can be red-shifted if a pseudostilbenyl fragment which is *p*-substituted with an EWG is included in the structure.[15] The D–A interaction *via* a conjugated system and the increase in the size of the π-spacer, result in the formation of a new low-energy molecular orbital and a decrease in the HOMO–LUMO gap.[14,15] With purpose of comparison, we included the spectra and optical parameters of compounds **2e–g** recently informed by our group.[15]

We observed that when a moderated electron-acceptor group such as –CF_3 or –CN is included in the *para*-position of the stilbenyl moiety, the main absorption band does not display important changes in comparison to **2e**. Only in the case of a strong electron-withdrawing group such as a –NO_2 group, a larger intensity and a similar red-shift of both transition bands are observed (Table 4, entries 1, 2 and 6). In contrast, for the electron-releasing group –OMe, we also observe a red-shift, but it is less important than that exhibited by the

Table 3 Synthesis of azo-pyrrole dyes **4b–d**

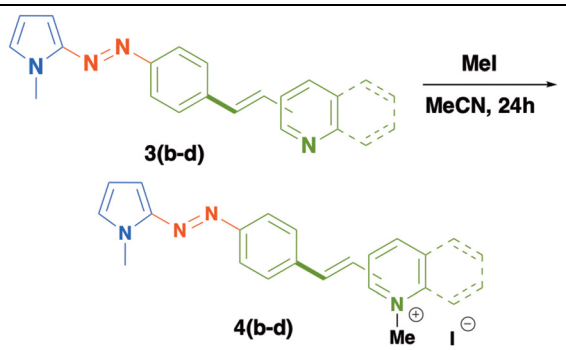

Entry	Compound	Het	Yield[a] (%)
2	**4b**	4-(*N*-Methylpyridinium)	90
3	**4c**	3-(*N*-Methylpyridinium)	95
4	**4d**	4-(*N*-Methyl quinolinium)	76

[a] Isolated yield after SiO_2 column chromatography.

Table 4 UV-Vis data for the pyrrole azo dyes **2a–d** acquired in MeOH and $CHCl_3$

			MeOH				$CHCl_3$						
Entry	Comp.	R	λ_{max} (nm)	E_{exp} (eV)	ε (10^4 cm^{-1} M^{-1})	E_{theo} (eV)[1]	λ_{max} (nm)	E_{exp} (eV)	ε (10^4 cm^{-1} M^{-1})	E_{theo} (eV)[2]	λ_{onset} (nm)[3]	Op. E_g (eV)[3]	Calc. E_{gap} (eV)[4]
1	**2a**	CF_3	415	2.99	4.08	3.16	419	2.96	3.36	3.10	497	2.50	1.92
2	**2b**	CN	419	2.96	3.42	3.11	423	2.94	3.30	3.07	500	2.48	1.87
3	**2c**	Br	415	2.99	4.08	3.14	420	2.96	3.53	3.10	499	2.49	1.91
4	**2d**	OMe	421	2.94	3.74	3.09	424	2.93	3.25	3.06	506	2.45	1.81
5	**2e**	H	402	3.08	3.49	3.14	415	2.99	3.07	3.11	502	2.47	1.94
6	**2f**	NO_2	426	2.91	5.65	3.04	431	2.88	4.01	3.03	511	2.43	1.64
7	**2g**	NMe_2	460	2.70	4.99	2.90	467	2.66	3.34	2.90	539	**2.30**	**1.48**

Calculated excitation energies obtained from the computed absorption spectra in [1]MeOH and [2]$CHCl_3$ at the CAM-B3LYP/Def2-TZVP level of theory using MeOH and $CHCl_3$ as implicit solvent (SMD model). [3]Data obtained from experimental UV-visible spectra acquired in MeOH. [4]Frontier molecular orbitals in the minimum energy orientation for the *E* isomers calculated with the PBE/cc-pVDZ level of theory using MeOH as implicit solvent (SMD model).

–NMe_2 group[15] (Table 4, entries 4 and 7). We also acquired the absorption spectra of compounds **3a–d** and **4b–d** in methanol (Fig. 2 and 3). Systems **3a–d** display a similar behavior as the series of push–pull azodyes **2a–d**, with a slight red-shift in comparison to **2e**.

With respect to **3a**, the inclusion of the ferrocenyl group which behaves like an electron releasing group gave rise to additional absorptions bands between 400 and 600 nm as result of n–π* transitions and an MLCT absorption of the ferrocenyl group.[20] However, when we compare the absorption spectra of **3b–d** with those of compounds **4b–d**, we noticed that the methylation of the nitrogen atom included in these azo-pyrrole dyes induces an important bathochromic effect and increases the intensity of the absorption (ε), in comparison to their neutral counterparts **3b–d** and **2e**. This observation confirms that the insertion of a stronger electron withdrawing group such as a pyridinium or quinolinium salt helps to generate zwitterionic resonance structures that contributes to decrease the energy of the excited state (Scheme 2).[21] This

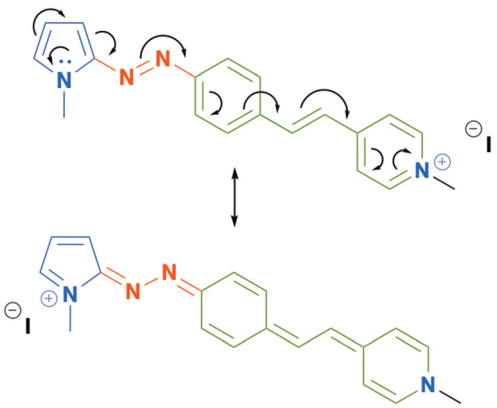

Scheme 2 Zwitterionic resonance structures of compound **4b**.

behavior is less important in compound **4c**, and hence, the smaller red-shift of its main absorption band. This circumstance occurs because the 3-pyridinium moiety acts as an electron-acceptor group only by inductive effects (Table 5, entry 6).

Optical energy Gap. The E_{GAP} value can be correlated with the excitation energy corresponding to a particular absorption by means of the relation,

$$E = h\nu = hc/\lambda. \quad (1)$$

Using the approximation of the first optical absorption edge calculated from UV-vis spectra of these compounds (Fig. S30, S35, S40, S45, S50, S55, S60, S65, S70, S75 and S80†), we estimated the energy difference between the HOMO–LUMO orbitals.[15,22] We used the optical absorption spectra of all samples acquired from MeOH solutions, and we compared them with the results obtained from computational studies (Tables 4 and 5) as discussed below.

Theoretical calculations. So as to gain further insight about the charge transfer properties of the azo-compounds studied in this work, we calculated the molecular structure for the series **2a–g**, **3a–d** and **4b–d** using the PBEh-3c approximation. The molecular structure predicted for **3b** agrees well with that determined by X-ray diffraction analysis.

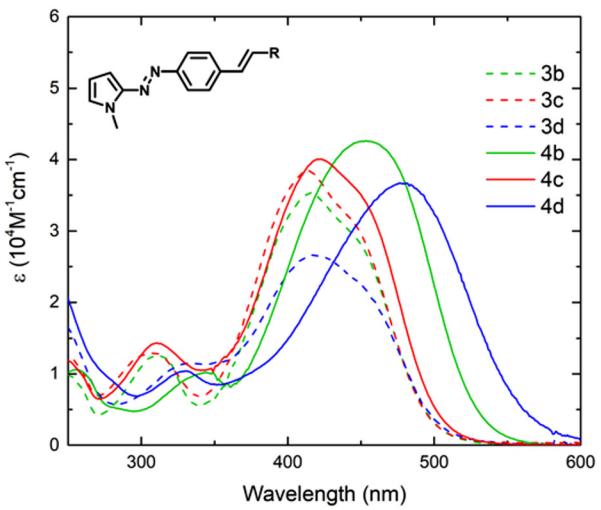

Fig. 3 Comparison of UV-Visible spectra of **3b–d** (dotted line) and **4b–d** (continue line) acquired in MeOH.

Table 5 UV-Vis data for pyrrole azo dyes **3a–d** and **4b–c** acquired in MeOH

			MeOH				$CHCl_3$						
Entry	Comp.	Het	λ_{max} (nm)	E_{exp} (eV)	ε (10^4 cm^{-1} M^{-1})	E_{calc} (eV)[1]	λ_{max} (nm)	E_{exp} (eV)	ε (10^4 cm^{-1} M^{-1})	E_{calc} (eV)[2]	λ_{onset} (nm)[3]	Op. E_{Gap} (eV)[3]	Calc. E_{gap} (eV)[4]
1	**3a**	Fc	413	3.00	3.00	3.28	415	2.99	3.12	3.28	560	2.21	1.50
2	**3b**	4-Py	416	2.98	3.61	3.17	418	2.97	4.10	3.13	498	2.49	1.92
3	**3c**	3-Py	414	2.99	3.92	3.16	417	2.98	2.53	3.12	499	2.49	1.94
4	**3d**	4-Quin	418	2.97	2.53	3.16	423	2.94	3.07	3.12	505	2.46	1.95
5	**4b**	4-Py(N)$^+$Me	454	2.73	3.98	3.03	—	—	—	2.83	531	2.37	1.63
6	**4c**	3-Py(N)$^+$Me	422	2.94	4.04	3.16	—	—	—	3.05	505	2.45	1.86
7	**4d**	4-Quin(N)$^+$Me	476	2.60	3.76	2.99	—	—	—	2.82	564	**2.20**	**1.56**

Calculated excitation energies obtained from the computed absorption spectra in [1]MeOH and [2]$CHCl_3$ at the CAM-B3LYP/Def2-TZVP level of theory using MeOH and $CHCl_3$ as implicit solvent (SMD model). [3]Data obtained from experimental UV-visible spectra acquired in MeOH. [4]Frontier molecular orbital in the minimum energy orientation for the *E* isomers calculated with the PBE/cc-pVDZ level of theory using MeOH as implicit solvent (SMD model).

Then, we calculated the energy values for the frontier orbitals HOMO/LUMO, and from those values, we also calculated the energy gap for all compounds (Tables 4 and 5). The HOMO and LUMO of all *E* isomers are clearly of π-nature. We observe a good trend in the obtained data, showing that the incorporation of a quinolinium moiety as EWG in **4d** favors a better push–pull character (Table 5, entry 7).

We computed the absorption spectrum of the compounds **2a–2g**, **3a–3d** and **4b–4d** in methanol [Fig. 4(a), (c) and (e)]. The error of the computed excitation energies is smaller than 0.3 eV in all cases (except for compound **4d** for which the difference between the computed and the experimentally determined excitation energies is 0.39 eV). The experimental trends are overall well reproduced. For example, (i) the general order of the excitation energies throughout the series **2a–2g** and **4b–4d** (although the calculated energy of **2g** is slightly smaller than that **2e**) and (ii) the closeness in the excitation energies of the compounds **3a–3d**. The calculations also predict in agreement with experiment that (i) the methylation of compounds **3b–3d** to generate systems **4b–4d** induces a bathochromic shift and (ii) the red-shift for the change **3c** to **4c** is the smallest one in this regard. We also computed similar results (Fig. 4(b) and (d)) for the excitation energies of the compounds in chloroform, concerning the ordering of the excitation energies and errors with respect to the values experimentally registered. In particular, the theoretical calculations also agree with the experimentally observed modest bathochromism when we change the solvent from methanol to chloroform. These experimental and theoretical results indicate that the electronic structure of the investigated chromophores does not change substantially because of photoexcitation. We exploited wavefunction analyses particularly the Quantum Theory of Atoms in Molecules (QTAIM)[23] to inquire further about this hypothesis. The QTAIM divides the 3D-space of an electronic system in atomic basins Ω_A,Ω_B... based on the topological properties of the electron density, which equals the expectation value of a Dirac observable, *viz.*,

$$\varrho(\boldsymbol{r}) = \left\langle \sum_{i=1}^{N} \delta(\boldsymbol{r} - \boldsymbol{r}_i) \right\rangle. \quad (2)$$

The QTAIM atoms are proper open quantum subsystems for which one may compute expectation values of different Dirac observables, for instance, the number of electrons within them, as

$$N(\Omega_A) = \int_{\Omega_A} \varrho(\boldsymbol{r}) \mathrm{d}\boldsymbol{r}, \quad (3)$$

to afterwards compute the QTAIM atomic charges,

$$Q(\Omega_A) = Z(\Omega_A) - N(\Omega_A), \quad (4)$$

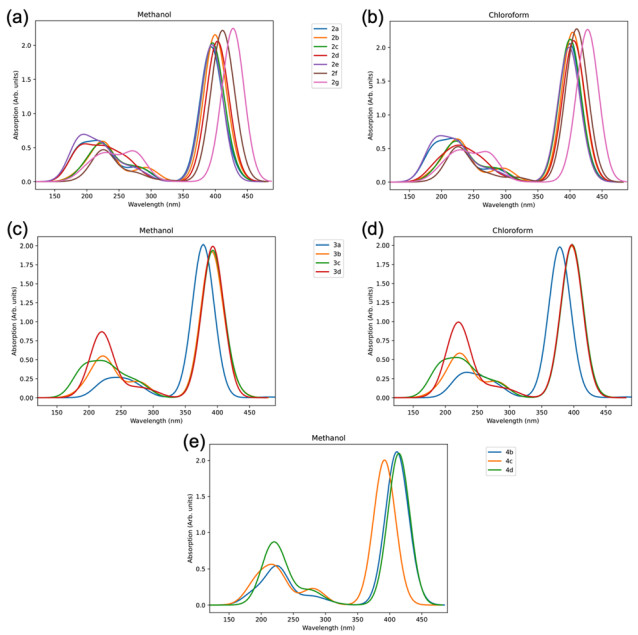

Fig. 4 Computed TDDFT absorption spectra of the compounds addressed in this investigation: (a) **2a–2g** in methanol, (b) **2a–2g** in chloroform, (c) **3a–3d** in methanol, (d) **3a–3d** in chloroform and (e) **4b–4d** in methanol.

in which $Z(\Omega_A)$ is the atomic number of the nucleus inside the QTAIM basin Ω_A. The QTAIM allows to compute atomic charges in different electronic states. Fig. 5 reports the values of:

$$\Delta Q(\Omega_A) = Q*(\Omega_A) - Q^{S_0}(\Omega_A) \quad (5)$$

for compounds **2a** and **3a** wherein $Q^*(\Omega_A)$ and $Q^{S_0}(\Omega_A)$ are the QTAIM charges of basin Ω_A in the computed excited bright state and the ground state, respectively. The computed values of $\Delta Q(\Omega_A)$ reveal that the charges of the QTAIM basins of the examined chromophores change only very slightly because of photoexcitation. Indeed, the changes in QTAIM charges satisfy the inequality $|\Delta Q(\Omega_A)| < 0.05$ a.u. The values of $\Delta Q(\Omega_A)$ for all the systems addressed herein are reported in the ESI.† The small modifications of $Q(\Omega_A)$ are consistent with the slight solvatochromic effect observed between methanol and chloroform as previously discussed.

Photoisomerization studies. We next studied the photoisomerization of these azo-pyrrole dyes upon irradiation into the first absorption band. For this purpose, a 2.5×10^{-5} M solution of these compounds in methanol was irradiated with a 5 W white led for 1 minute (time required to establish a photostationary state, PSS) at room temperature (Table 6).

The emission profile of the white LED exhibits two bands: a narrowband at 452 nm and a broad band in the range of 490–670 nm, which conform with the n–π* transition observed in all the azo-compounds studied allowing its use as an alternative of the common narrowband lasers (Fig. S81†).

The UV-vis spectra of **2a** and the corresponding PSS after irradiation, along with several intermediate spectra are showed in Fig. 6 (top). The exponential evolution for the *cis* → *trans* isomerization, obtained from the UV-vis data is presented in Fig. 6 (dawn). The corresponding UV-Vis measurements for the series **2b–d**, **3a–d** and **4b–d** are included in the ESI.† From the PSS spectra of ***Z*-2a** and the deconvolution of the *cis*/*trans* contributions, the absorption maxima for the *cis* isomer were identified at 312 and 346 nm. These absorption bands correspond to π–π* and n–π* transitions, respectively and they are blue-shifted due to the loss of conjugation in the azo compound. Likewise, we observe that the n–π* transition occurs with a higher molar absorptivity coefficient than that observed for the *E*-isomer. We also notice that azo-stilbenylpyrroles containing electron donor groups **2d**, **2g** and **3a** exhibit shorter half-life times and larger rate constants in comparison to the other members of this series.

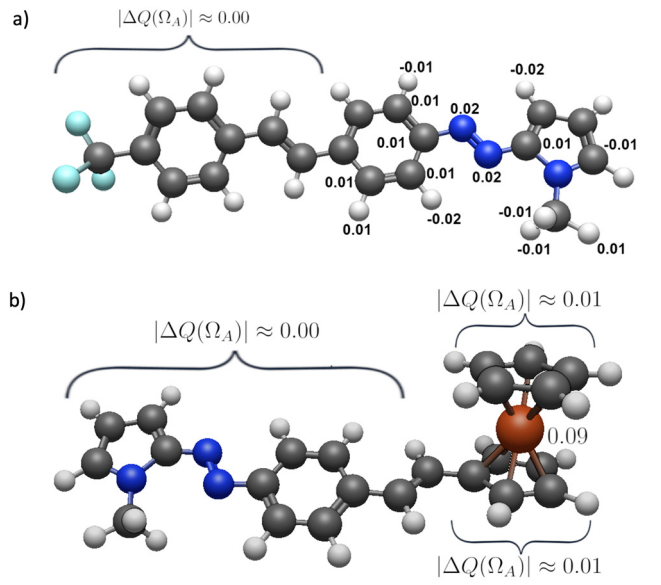

Fig. 5 Values of $\Delta Q(\Omega_A)$ (eqn (4)) for the QTAIM basins within compounds (a) **2a** and (b) **3a** addressed in this investigation.

Table 6 Half-life ($t_{1/2}$, min) rate constant (k, s^{-1}) cis-trans thermal isomerization, *cis*/*trans* percent in the photoisomerization state for the different compounds addressed in this investigation[a]

Entry	Compound	R	$t_{1/2}$ (min)	k (s^{-1})	PSS (%) *Z*	PSS (%) *E*
1	**2a**	CF_3	7.8	1.5×10^{-3}	74	26
2	**2b**	CN	6.6	1.7×10^{-3}	71	29
3	**2c**	Br	5.6	2×10^{-3}	70	30
4	**2d**	OMe	2.7	4.2×10^{-3}	71	29
5	**2e**	H	4.6	2.5×10^{-3}	72	28
			8.6[b]	1.3×10^{-3} [b]	72[b]	28[b]
6	**2f**	NO_2	9.4	1.2×10^{-3}	69	31
			12.1[b]	9.7×10^{-4} [b]	83[b]	17[a]
7	**2g**	NMe_2	3.4	3.3×10^{-3}	42	58
			4.4[b]	2.7×10^{-3} [b]	67[b]	33[b]
8	**3a**	Fc	2	5.5×10^{-3}	24	76
9	**3b**	4-Py	8.7	1.3×10^{-3}	72	28
10	**3c**	3-Py	8.7	1.3×10^{-3}	71	29
11	**3d**	4-Quin	5.8	1.9×10^{-3}	72	28
12	**4b**	4-Py(N)Me^+	5.4	2.1×10^{-3}	66	34
13	**4c**	3-Py(N)Me^+	7.8	1.5×10^{-3}	73	27
14	**4d**	4-Quin(N)Me^+	0.8	1.2×10^{-3}	45	55

[a] UV-Vis spectra acquired in MeOH at 2×10^{-5} M, $E \rightarrow Z$ PSS irradiation conducted with a white led at RT. [b] These data were acquired at 20 °C upon irradiation at 485 nm, using a pulsed laser.[15]

On the other hand, the azo-compounds **3b–d**, which include π-deficient heteroaryls, show longer half-life times than those of **2a** and **2b**. The behavior of these compounds changes when the electron withdrawing character in these compounds is increased after nitrogen alkylation (**4b–d**). Likewise, we observe that the incorporation of a 4-quinoline moiety in **3d** and **4d** also modifies the kinetic parameter of the photoisomerization process. This circumstance can be attributed to the extended electronic delocalization of this fragment and the high stability of the hydrazo tautomer that enhances the rotation across the single N–N bond (Scheme 3). In general, we observe that the inclusion of a NO_2 group as part of the push–pull stilbenyl-azopyrrole **2g** increases the thermal stability of the *cis*-isomer, a condition which leads to the best photoisomerization yield.

To probe the photostability of all these compounds upon several irradiation-relaxation cycles, we prepared methanolic solutions of the series ***E*-2(a–d)**, ***E*-3(a–d)** and ***E*-4(b–d)**, which

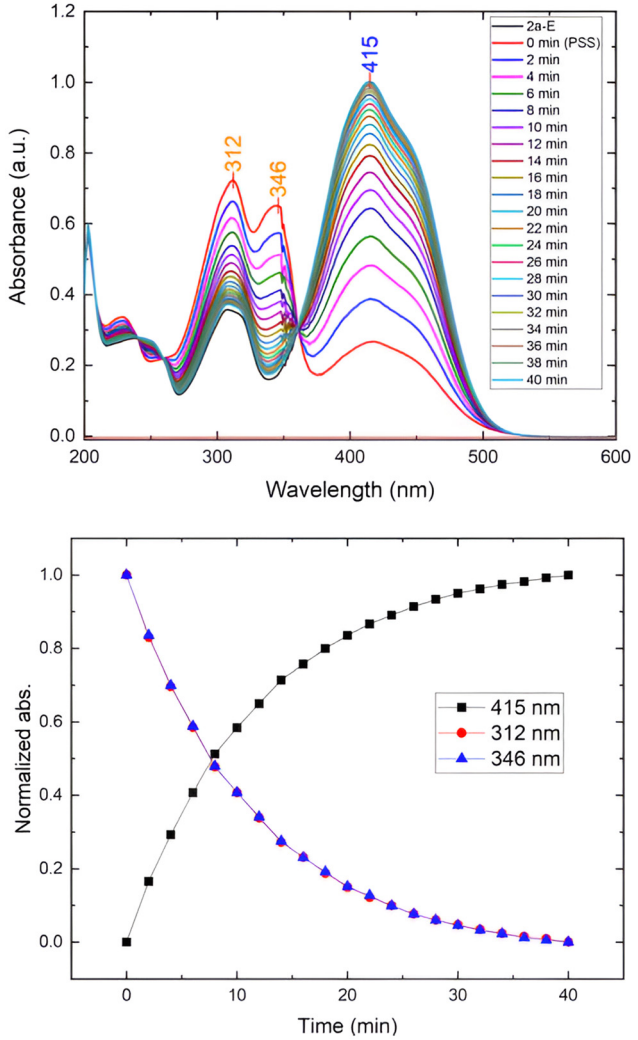

Fig. 6 (Top) UV-vis absorption spectra for **2a** in the photo-stationary state after white led irradiation, and spectral evolution during the *cis* → *trans* thermal return. (Dawn) Absorption changes during the *cis* → *trans* thermal return at three different wavelengths.

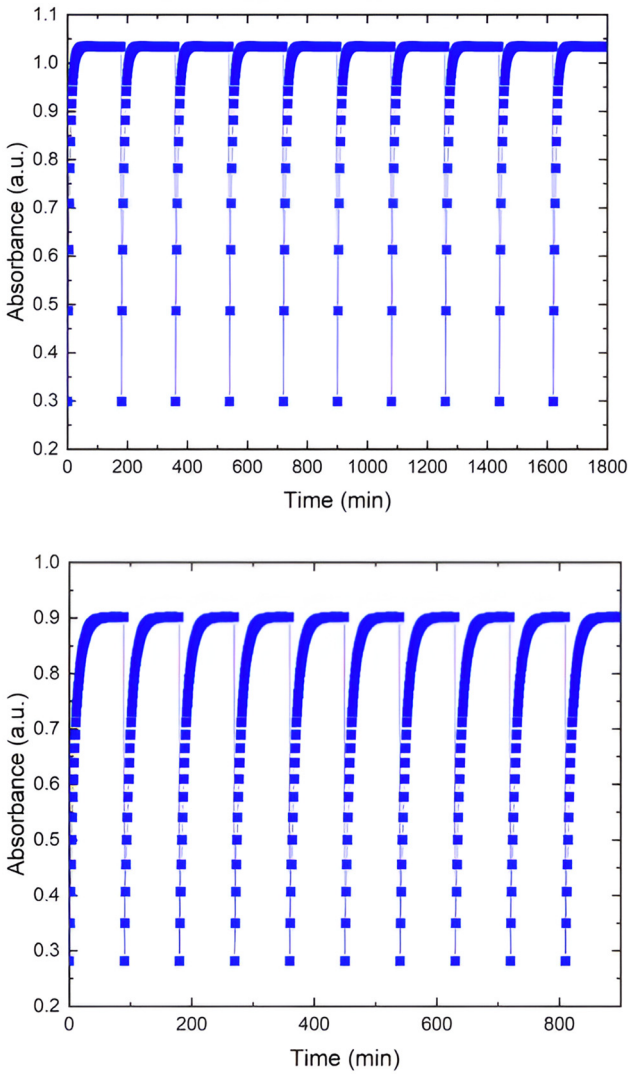

Fig. 7 Photoisomerization fatigue cycles for compounds **2a** (top) and **4b** (dawn). Samples were irradiated ten times for 2 minutes (5.0 mW).

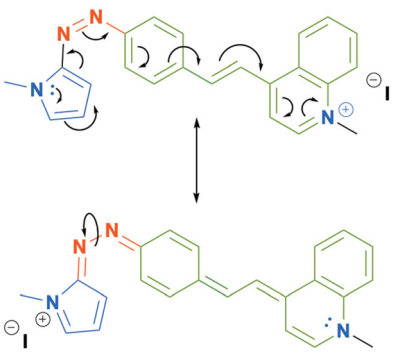

Scheme 3 Resonance structures of the azo-compound **4d**.

were exposed at least to ten irradiation-relaxation cycles using white led irradiation. These azo-compounds do not show any appreciable photobleaching (Fig. 7 and S29–S79 in the ESI†).

Aggregation studies. We recently demonstrated that push–pull byphenylazo-pyrroles compounds present aggregation in solution. This aggregation modifies their optical properties due to formation of J-aggregates.[14] More specifically, J-aggregates are characterized by an arrangement of monomeric molecules in one dimension to achieve an anti-parallel orientation of their transition moments with a zero angle between the transition moments and the line joining the molecular centers.[24] This behavior is easily recognized by the presence of an inflection at the right of the π–π* absorption band of the associated chromophore.[25]

As the synthesized stilbenyl azopyrroles showed limited solubility in water, we can force their arrangement forming aggregates in partially aqueous medium and we can examine the system *via* UV/visible absorption spectroscopy.[26] To study this possible aggregation process, we used MeOH : H_2O as a binary solvent at the same sample concentration.

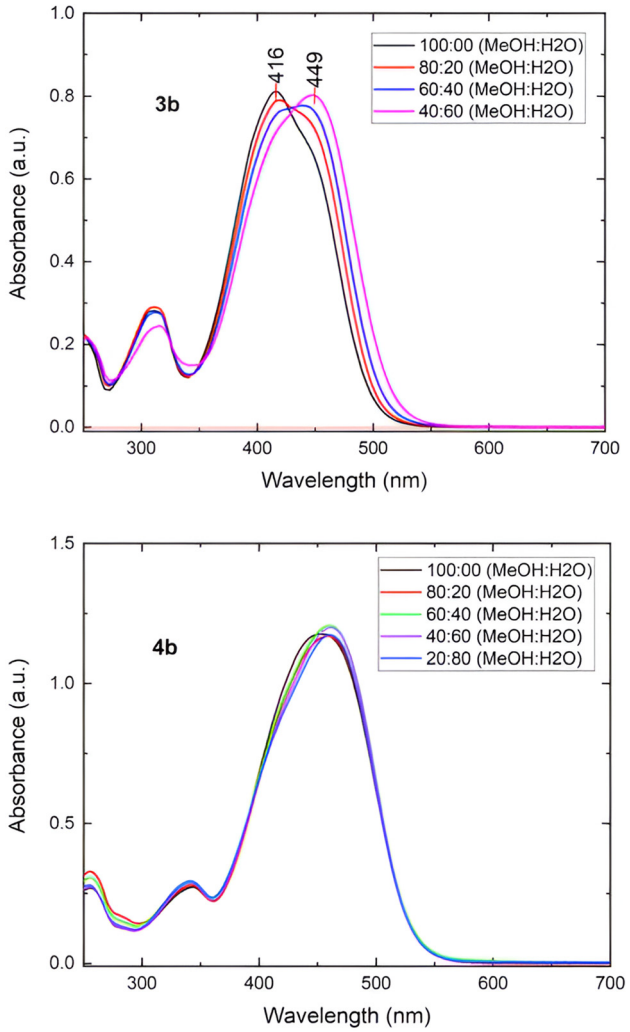

Fig. 8 (Top) UV-visible spectra of compound **3b** in different ratios MeOH/H_2O. (Dawn) UV-visible spectra of compound **4b** in different ratios MeOH/H_2O.

The results obtained for **3b** and **4b** are shown in Fig. 8. For instance, **3b** exhibits a main absorption band at λ_{max} = 416 nm, but when the proportion of water increases, the absorption band adopts an asymmetrical shape with a slight inflexion around 456 nm, showing a clear isosbestic point, suggesting the formation of J-aggregates.[24b] A similar behavior is observed for **3c** and **3d**. This behavior agreed with the molecular arrangement observed in the solid state of this compound analyzed by X-ray diffraction (Fig. 1).

Likewise, to gain further insights about this behavior, we calculated the association energies of a head-to tail **3b**-dimer, as a reduced model of a J-aggregate, in methanol and water (Table 7 and Fig. 9). The calculated values reveal that this compound exhibits a significant tendency to aggregate in an antiparallel form in polar solvents.

When we explored the aggregation behavior of **4b–d** in the same conditions, we only detected a slight bathochromic effect as result of the increase in the binary solvent polarity, characteristic of these push–pull azo-pyrrole compounds.[14]

Table 7 Association energies calculated for the **3b**-dimer[a]

Entry	Solvent	E_{as} (kcal mol^{-1})
1	MeOH	12.5
2	H_2O	7.9

[a] Association energies (E_{as}) computed at the CAM-B3LYP/Def2-TZVP level of theory.

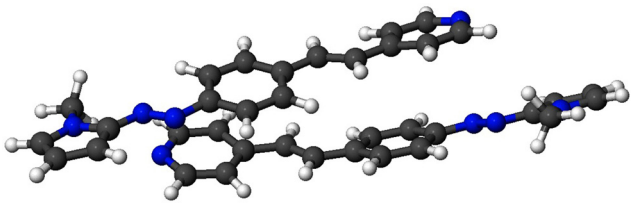

Fig. 9 Optimization of the calculated head-to-tail dimer of **3b** in MeOH.

Finally, we studied the photoisomerization of **3b**, using MeOH/water (80 : 20) as a binary solvent. After illumination with the white led for 1 minute, we observed a very fast thermal relaxation from the PSS to the *trans*-isomer, to the extent that we could not record kinetic parameters (Fig. 10). This behavior is consistent with the formation of J-aggregates and it also indicates that the thermal relaxation can be water-assisted. A similar behavior was observed in their closely related biphenyl-azopyrroles, which displayed smaller photoisomerization rate constant and thermal half-lives in these conditions.[14] As we stated before, some azo-heteroaryl compounds have been used as photopharmaceutical agents.[7f,9b] In this kind of applications, the use of a physiological medium mainly composed by water can promote the formation of aggregates, modifying the photoisomerization kinetics of these compounds as we have demonstrated in previous reports.[14]

Experimental

General considerations

All reagents and solvents were obtained from commercial suppliers and used without further purification. Column chromatography was performed using 70–230 mesh silica gel.

All compounds were characterized by IR spectra, recorded on a Perkin-Elmer Spectrum 100 FT-IR equipped with ATR accessory, and all data are expressed in wave numbers (cm^{-1}). Melting points were obtained on a Stuart Melting Point Apparatus SMP10 and are uncorrected. NMR spectra were measured with a Bruker Avance III at 300 MHz for ^{1}H and 75 MHz for ^{13}C using $CDCl_3$, and DMSO-d_6, as solvents. Chemical shifts are in ppm (δ), relative to TMS. The MS-FAB spectra were obtained on a JMS-SX102A spectrometer using nitrobenzyl alcohol and polyethylene glycol matrices.

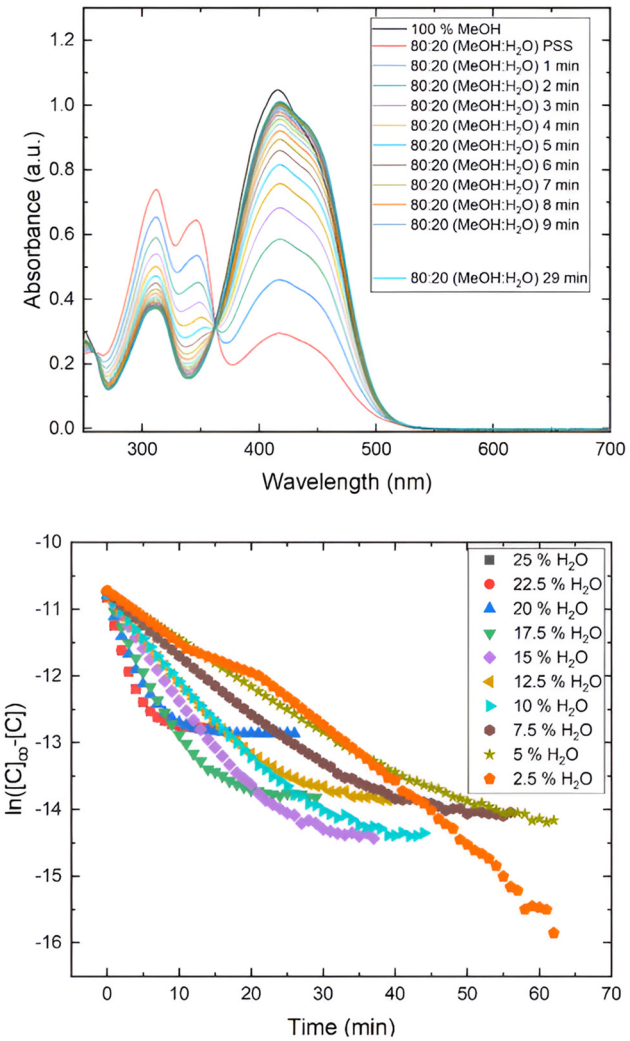

Fig. 10 (Top) UV-Vis spectra for **3b** (2.9×10^{-5} M, MeOH/H_2O 80 : 20) after irradiation (PSS) and *cis–trans* return. The spectra were acquired every minute. (Dawn) $\ln([C]_\infty - [C])$ *vs.* time for **3b** (2.9×10^{-5} M) after white light irradiation in different ratios MeOH/H_2O (the loss of linearity is observed).

MS-DART spectra were obtained on an AccuTOF JMS-T100LC spectrometer. The values of the signals are expressed in mass/charge units (m/z).

UV-Vis absorption spectra were recorded at 298 K on a Thermo-Scientific Evolution 60S UV-Vis spectrophotometer, using spectrophotometric grade solvents purchased from Sigma-Aldrich Co. and 1 cm quartz cell. The solvatochromic study was performed using 10^{-5} M to 10^{-4} M solutions of azopyrrole dyes in $CHCl_3$ and MeOH as solvents at room temperature.

The aggregation study was carried out using 5×10^{-5} M solutions of azopyrrole dyes at different MeOH : H_2O ratios, from 100 : 0 to 20 : 80 at room temperature. ASTM type 1 ultrapure water (Millipore-Q system, 18.2 MΩ cm) was used as solvent for the aggregation studies.

Isomerization kinetic measurements. UV-vis absorption spectra were recorded in a Thermo-Scientific Evolution 60S spectrometer. The solvent used for all experiments was methanol HPLC grade (Sigma Aldrich). The photoisomerization reaction was induced by irradiation using a 5 W white led, which displays two emission bands, a narrow one at 452 nm and other in the range of 490–670 nm (Fig. S81†). Solutions of the studied compounds were irradiated under continuous stirring in a quartz cell with 1 cm of optical pathway.

Structure determination by X-ray crystallography. Suitable X-ray-quality crystals of **3b** were grown by slow evaporation of a mixture of dichloromethane/hexane at room temperature. A crystal of **3b** was mounted on a glass fiber at room temperature and then placed on a Bruker Smart Apex CCD equipped with Mo-Kα radiation. The decay was negligible in all cases. Details of crystallographic data collected for compound **3b** are provided in the ESI.† Systematic absences and intensity statistics were used in space group determination. The structure was solved using direct methods.[27] Anisotropic structure refinements were achieved using full matrix, least-squares technique on all non-hydrogen atoms. All hydrogen atoms were placed in idealized positions, based on hybridization, with isotropic thermal parameters fixed at 1.2 times the value of the attached atom. Structure solutions and refinements were performed using SHELXTL V6.10.[28] The experimental and refinement details of the X-ray crystallographic structure of compounds **3b**, CCDC 2189449.†[29]

Computational studies

We used the ORCA program[30] to compute the structures of molecules at the PBEh-3c level of theory.[31] The HOMO–LUMO gaps were computed using the PBE/cc-pVDZ approximation as this functional has been successfully exploited for this purpose previously in our group.[14] Subsequently, TDDFT calculations were carried out using the range-separated CAM-B3LYP functional[32] and the Def2-TZVP basis set.[33] The SMD approach[34] was employed to consider solvent effects due to methanol and chloroform. Finally, we performed QTAIM wave function analyses with the aid of the AIMAll software package[35] over DFT densities obtained using the GAUSSIAN software[36] following the procedure detailed in ref. 37. Finally, we used the Avogadro program for visualization.[38]

Synthetic procedures

Synthesis of compound 1. In a 100 mL round-flask, 4-iodoaniline (2.51 g, 11.2 mmol) and *N*-methylpyrrole (1 mL, 11.2 mmol), were dissolved in 6 mL of MeOH, then HCl [1 M] (10 mL, 0.01 mol) was added and the mixture was cooled at mixed at 0 °C. Then, an aqueous solution of sodium nitrite (0.93 g, 13.4 mmol in the minimum possible quantity of water) was added dropwise. The mixture was stirred for 10 minutes at 0 °C and then for 30 more minutes at room temperature. A solution of 10% NaOH was added until pH = 10 was reached and then, the mixture was extracted with CH_2Cl_2 and dried with anhydrous Na_2SO_4. The crude product was purified by

column chromatography on silica gel with hexane. The spectroscopic data agreed with those reported in the literature.[13,14]

Synthesis of vinyl arenes. In a 100 mL round flask were added 1 g of the corresponding aldehyde, 1.2 equiv. of methyl triphenylphosphonium bromide and 2 equiv. of K_2CO_3 in 40 mL of THF. The mixture reaction was refluxed for 12 h. Afterwards, the solvent was removed by a reduced pressure distillation and the crude was redissolved in 20 mL of dichloromethane, washed with water (2 × 20 mL) and dried with anhydrous Na_2SO_4. The crude product was purified by column chromatography on silica gel with hexane. All vinyl arenes synthesized were characterized by NMR and the corresponding spectra are accordant with the literature.[39]

Synthesis of stilbenyl-azopyrroles 2a–d and 3a–d. A 10 mL vial was filled with compound **1** (0.5 mmol), triethylamine (0.75 mmol), the corresponding vinyl arene (0.6 mmol), 5 mL of DMF as solvent and 0.1% mol of the palladium complex as indicated in Table 1.[17] The vial was introduced into a stainless-steel reactor and placed in an oil bath at 160 °C. After the reaction had been completed, the reactor was cooled to room temperature, the system was decompressed, and the mixture of reaction was passed through a 2 cm celite column using ethyl acetate as solvent. Subsequently, the combined solvents were removed by high vacuum distillation. The crude was purified by chromatography on silica gel using hexane–AcOEt.

Synthesis of compounds 4b–d. In a 50 mL round-flask were added 0.5 mmol of the compound **3** and 5 equiv. of MeI in 10 mL of acetonitrile. The mixture was stirred for 24 h yielding a dark red solid. The solvent was eliminated by distillation under vacuo and the remanent solid was washed at least three times with diethyl ether and recovered by decantation.

Conclusions

We have successfully synthetized a new family of push–pull stilbenyl azopyrrole dyes **2a–g** and **3a–d** using a Heck–Mizoroki cross-coupling reaction in moderated to good yields. The exploited [Pd/(*N*,*N*)-pyrrole ligand] complex was an efficient and robust catalyst for this cross-coupling reaction using compound **1** in combination with diverse vinyl arenes. The alkylation reaction over the nitrogen of pyridine or quinoline moieties in azodyes **3b–d** induced an important red-shift to the visible region for the main absorption band.

The theoretical studies showed that the stilbenyl-azopyrroles including an efficient EWG as part of the push–pull system (**3d** *vs.* **4d**) have relatively low optical gaps energies and an effective electronic transfer, as result of the coplanarity across the π-system in the ground state. Likewise, stilbenyl-azopyrrole compounds can be photoisomerized upon irradiation into the first absorption band using a white led. We observe that the incorporation of a 4-quinoline moiety in **3d** and **4d** modifies the kinetic parameter of the isomerization process, which can be attributed to the extended electronic delocalization of this fragment and the high stability of the hydrazo tautomer that enhances the rotation across the single N–N bond. This behavior can be exploited for tunning the photoisomerization of the azo-compound. We have also demonstrated that these compounds can be auto-ensembled forming J-aggregates in binary-solvents as MeOH/water, and this behavior is consistent with that observed in the solid state. Indeed, we are confident that these findings will be useful to broaden the uses of these push–pull azo-switches in water compatible applications.

Conflicts of interest

There are no conflicts to declare.

Acknowledgements

Authors acknowledge UNAM for PAPIIT IN216123 and CONAHCYT for the Master. Sc. grant extended to D. G.-R. (887548). The authors are thankful to DGTIC-UNAM for computer time (project LANCAD-DGTIC-UNAM-250). We thank the technical assistance provided by Cesar I. Sandoval Chávez, Martin Cruz Villafañe and M. C. García-González.

References

1 (*a*) R. Costil, M. Holzheimer, S. Crespi, N. A. Simeth and B. L. Feringa, *Chem. Rev.*, 2021, **121**, 13213–13237; (*b*) D. Dattler, G. Fuks, J. Heiser, E. Moulin, A. Perrot, X. Yao and N. Giuseppone, *Chem. Rev.*, 2020, **120**, 310–433.
2 J. M. Abendroth, O. S. Bushuyev, P. S. Weiss and C. J. Barrett, *ACS Nano*, 2015, **9**, 7746–7768.
3 (*a*) S. Chen, R. Costil, F. K.-C. Leung and B. L. Feringa, *Angew. Chem., Int. Ed.*, 2021, **60**, 11604–11627; (*b*) Z. Yu and S. Hecht, *Chem. Commun.*, 2016, **52**, 6639–6653; (*c*) J. Vapaavuori, C. G. Bazuin and A. Priimagi, *J. Mater. Chem. C*, 2018, **6**, 2168–2188; (*d*) D.-H. Qu, Q.-C. Wang, Q.-W. Zhang, X. Ma and H. Tian, *Chem. Rev.*, 2015, **115**, 7543–7588.
4 (*a*) A. Telleria, P. W. N. M. van Leeuwen and Z. Freixa, *Dalton Trans.*, 2017, **46**, 3569–3578; (*b*) T. Imahori, R. Yamaguchi and S. Kurihara, *Chem. – Eur. J.*, 2012, **18**, 10802–10807; (*c*) R. S. Stoll and S. Hecht, *Angew. Chem., Int. Ed.*, 2010, **49**, 5054–5075.
5 Selected references: (*a*) G. Campillo-Alvarado, R. J. Liu, D. W. Davies and Y. Diao, *Cryst. Growth Des.*, 2021, **21**, 3143–3147; (*b*) J. Long, D. Kumar, C. Deo, P. Retailleau, G. V. Dubacheva, G. Royal, J. Xie and N. Bogliotti, *Chem. – Eur. J.*, 2021, **27**, 9563–9570; (*c*) E. M. Bolitho, H. E. Bridgewater, R. J. Needham, J. P. C. Coverdale, P. D. Quinn, C. Sanchez-Cano and P. J. Sadler, *Inorg. Chem. Front.*, 2021, **8**, 3675–3685; (*d*) B. Peng, H. Li, Y. Li, Z. Lv, M. Wu and C. Zhao, *Chem. Eng. J.*, 2020, **395**, 125079; (*e*) S. Maity, K. Naskar, T. Bhowmik, A. Bera, T. Weyhermüller, C. Sinha and P. Ghosh, *Dalton Trans.*, 2020, **49**, 8438–8442.

6 Selected references: (*a*) D. M. Adrion, D. S. Kaliakin, P. Neal and S. A. Lopez, *J. Phys. Chem. A*, 2021, **125**, 6474–6485; (*b*) M. X. He, Y.-Z. Wu, Y. Yao, Z.-Y. Mo, Y.-M. Pan and H.-T. Tanga, *Adv. Synth. Catal.*, 2021, **363**, 2752–2756; (*c*) T.-T. Yin, Z.-X. Zhao and H.-X. Zhang, *New J. Chem.*, 2017, **41**, 1659–1669; (*d*) J. Chen and Z. Yin, *Dyes Pigm.*, 2014, **102**, 94–99; (*e*) J. Calbo, C. E. Weston, A. J. White, H. S. Rzepa, J. Contreras-Garcia and M. J. Fuchter, *J. Am. Chem. Soc.*, 2017, **139**, 1261–1274; (*f*) C. E. Weston, R. D. Richardson, P. R. Haycock, A. J. White and M. J. Fuchter, *J. Am. Chem. Soc.*, 2014, **136**, 11878–11881.

7 Selected references: (*a*) Z.-Y. Zhang, Y. He, Y. Zhou, C. Yu, L. Han and T. Li, *Chem. – Eur. J.*, 2019, **25**, 13402–13410; (*b*) J. Calbo, A. R. Thawani, R. S. L. Gibson, A. J. P. White and M. J. Fuchter, *Beilstein J. Org. Chem.*, 2019, **15**, 2753–2764; (*c*) S. Vela, C. Krüger and C. Corminboeuf, *Phys. Chem. Chem. Phys.*, 2019, **21**, 20782–20790; (*d*) S. Devi, M. Saraswat, S. Grewal and S. Venkataramani, *J. Org. Chem.*, 2018, **83**, 4307–4322; (*e*) L. Stricker, M. Böckmann, T. M. Kirse, N. L. Doltsinis and B. J. Ravoo, *Chem. – Eur. J.*, 2018, **24**, 8639–8647; (*f*) C. E. Weston, A. Kramer, F. Colin, Ö. Yildiz, M. G. J. Baud, F.-J. Meyer-Almes and M. J. Fuchter, *ACS Infect. Dis.*, 2017, **3**, 152–161.

8 (*a*) C. Schütt, G. Heitmann, T. Wendler, B. Krahwinkel and R. Herges, *J. Org. Chem.*, 2016, **81**, 1206–1215; (*b*) G. Heitmann, C. Schütt and R. Herges, *Eur. J. Org. Chem.*, 2016, 3817–3823; (*c*) T. Wendler, C. Schütt, C. Näther and R. Herges, *J. Org. Chem.*, 2012, **77**, 3284–3287; (*d*) J. Otsuki, K. Suwa, K. K. Sarker and C. Sinha, *J. Phys. Chem. A*, 2007, **111**, 1403–1409; (*e*) J. Otsuki, K. Suwa, K. Narutaki, C. Sinha, I. Yoshikawa and K. Araki, *J. Phys. Chem. A*, 2005, **109**, 8064–8069.

9 (*a*) S. A. M. Steinmüller, D. Prischich, M. Odaybat, G. Galli, M. J. Fuchter and M. Decker, *Chem. Sci.*, 2024, **15**, 5360–5367; (*b*) S. A. M. Steinmuller, J. Fender, M. H. Deventer, A. Tutov, K. Lorenz, C. P. Stove, J. N. Hislop and M. Decker, *Angew. Chem., Int. Ed.*, 2023, **62**, e202306176.

10 (*a*) C. Boga, S. Cino, G. Micheletti, D. Padovan, L. Prati, A. Mazzanti and N. Zanna, *Org. Biomol. Chem.*, 2016, **14**, 7061–7068; (*b*) M. M. M. Raposo, M. C. R. Castro, M. Belsley and A. M. C. Fonseca, *Dyes Pigm.*, 2011, **91**, 454–465.

11 (*a*) J. Garcia-Amorós, B. Maerz, M. Reig, A. Cuadrado, L. Blancafort, E. Samoylova and D. Velasco, *Chem. – Eur. J.*, 2019, **25**, 7726–7732; (*b*) U. Daswani, U. Singh, P. Sharma and A. Kumar, *J. Phys. Chem. C*, 2018, **122**, 14390–14401; (*c*) J. Garcia-Amorós, M. C. R. Castro, P. Coelho, M. M. M. Raposo and D. Velasco, *Chem. Commun.*, 2013, **49**, 11427–11429; (*d*) M. C. R. Castro, P. Schellenberg, M. Belsley, A. M. C. Fonseca, S. S. M. Fernandes and M. M. M. Raposo, *Dyes Pigm.*, 2012, **95**, 392–399; (*e*) H. Faustino, C. R. Brannigan, L. V. Reis, P. F. Santos and P. Almeida, *Dyes Pigm.*, 2009, **83**, 88–94.

12 (*a*) N. A. Simeth, A. Bellisario, S. Crespi, M. Fagonnni and B. König, *J. Org. Chem.*, 2019, **84**, 6565–6575; (*b*) S. Crespi, N. A. Simeth, A. Bellisario, M. Fagnoni and B. König, *J. Phys. Chem. A*, 2019, **123**, 1814–1823; (*c*) N. A. Simeth, S. Crespi, M. Fagnoni and B. König, *J. Am. Chem. Soc.*, 2018, **140**, 2940–2946.

13 (*a*) J. Geng, Y. Dai, H. F. Qian, N. Wang and W. Huang, *Dyes Pigm.*, 2015, **117**, 133–140; (*b*) A. C. Razus, L. Birzan, M. Cristea, V. Tecuceanu and C. Enache, *Dyes Pigm.*, 2012, **92**, 1166–1176; (*c*) M. M. M. Raposo, A. M. F. P. Ferreira, M. Amaro, M. Belsley and J. C. V. P. Moura, *Dyes Pigm.*, 2009, **83**, 59–65.

14 J. A. Balam-Villarreal, B. J. López-Mayorga, R. A. Toscano, M. P. Carreón-Castro, V. Basiuk, F. Cortés-Guzmán, J. G. López-Cortés and M. C. Ortega-Alfaro, *Org. Biomol. Chem.*, 2020, **18**, 1657–1670.

15 L. Muñoz Rugeles, D. Gallardo-Rosas, J. Durán-Hernández, R. López-Arteaga, R. A. Toscano, N. Esturau-Escofet, J. G. López Cortés, J. Peon Peralta and M. C. Ortega Alfaro, *ChemPhotoChem*, 2020, **4**, 144–154.

16 (*a*) M. C. R. Castro, M. Belsey and M. M. M. Raposo, *Dyes Pigm.*, 2016, **128**, 89–95; (*b*) F. Bures, *RSC Adv.*, 2014, **4**, 58826–58861; (*c*) G. S. He, L.-S. Tan, Q. Zheng and P. N. Prasad, *Chem. Rev.*, 2008, **108**, 1245–1330.

17 E. Villatoro, L. Muñoz-Rugeles, J. Durán-Hernández, B. Salcido, N. Esturau-Escofet, J. G. López-Cortés, M. C. Ortega-Alfaro and J. Peón, *Chem. Commun.*, 2021, **57**, 3123–3126.

18 F. Hochberger-Roa, S. Cortés-Mendoza, D. Gallardo-Rosas, R. A. Toscano, M. C. Ortega-Alfaro and J. G. López-Cortés, *Adv. Synth. Catal.*, 2019, **361**, 4055–4064.

19 H. M. D. Bandara and S. C. Burdette, *Chem. Soc. Rev.*, 2012, **41**, 1809–1825.

20 (*a*) N. V. Pilipchuk, G. O. Kachkovsky, L. Slominskii Yu and O. D. Kachkovsky, *Dyes Pigm.*, 2006, **71**, 1–9; (*b*) B. López-Mayorga, C. I. Sandoval-Chávez, P. Carreón-Castro, V. M. Ugalde-Saldívar, F. Cortés-Guzmán, J. G. López-Cortés and M. C. Ortega-Alfaro, *New J. Chem.*, 2018, **42**, 6106–6113.

21 H. Meier, *Angew. Chem., Int. Ed.*, 2005, **44**, 2482–2506.

22 (*a*) J. C. S. Costa, R. J. S. Taveira, C. F. R. A. C. Lima, A. Mendes and L. M. N. B. F. Santos, *Opt. Mater.*, 2016, **58**, 51–60; (*b*) T. Michinobu, C. Boudon, J. P. Gisselbrecht, P. Seiler, B. Frank, N. N. P. Moonen, M. Gross and F. Diederich, *Chem. – Eur. J.*, 2006, **12**, 1889–1905.

23 R. F. W. Bader, *Atoms in Molecules: A Quantum Theory*, Oxford University Press, 1990.

24 (*a*) P. W. Bohn, *Annu. Rev. Phys. Chem.*, 1993, **44**, 37–60; (*b*) K. S. Kumar and A. Patnaik, *Chem. – Eur. J.*, 2011, **17**, 5327–5343.

25 (*a*) J. Jin, L. S. Li, Y. J. Zhang, Y. Q. Tian, S. Jiang, Y. Zhao, Y. Bai and T. J. Li, *Langmuir*, 1998, **14**, 5231–5236; (*b*) Z. Chen, C. Zhong, Z. Zhang, Z. Li, L. Niu, Y. Bin and F. Zhang, *J. Phys. Chem. B*, 2008, **112**, 7387–7394.

26 M. Kasha, *Radiat. Res.*, 1963, **20**, 55–71.

27 A. Altomare, G. Cascarano, C. Giacovazzo, A. Guagliardi, M. C. Burla, G. Polidori and M. Canalli, *J. Appl. Crystallogr.*, 1994, **27**, 435–436.

28 G. M. Sheldrick, *Acta Crystallogr., Sect. A: Found. Crystallogr.*, 2008, **64**, 112–122.
29 Crystal data of **3b**: $C_{18}H_{16}N_4$, M = 288.35, monoclinic, a = 11.0543(16), b = 7.6061(11), c = 18.348(3) Å, V = 1529.3(4) Å^3, T = 298 K, space group $P2_1$, Z = 4, μ(Mo-Kα) = 0.077 mm^{-1}, 8576 reflections measured, 3932 unique (R_{int} = 0.0604) (which were used in all calculations. The final R and wR(F^2) were 0.1570 and 0.1398 respectively (all data), CCDC 2189449.†
30 F. Neese, F. Wennmohs, U. Becker and C. Riplinger, *J. Chem. Phys.*, 2020, **152**, 224108.
31 S. Grimme, J. G. Brandenburg, C. Bannwarth and A. Hansen, *J. Chem. Phys.*, 2015, **143**, 054107.
32 T. Yanai, D. P. Tew and N. C. Handy, *Chem. Phys. Lett.*, 2004, **393**, 51–57.
33 F. Weigend and R. Ahlrichs, *Phys. Chem. Chem. Phys.*, 2005, **7**, 3297–3305.
34 A. V. Marenich, C. J. Cramer and D. J. Truhlar, *J. Phys. Chem. B*, 2009, **113**, 6378–6396.
35 T. A. Keith, *AIMAll (Version 19.10.12)*, TK Gristmill Software, Overland Park KS, USA, 2019 (**https://aim.tkgristmill.com**).
36 M. J. Frisch, G. W. Trucks, H. B. Schlegel, G. E. Scuseria, M. A. Robb, J. R. Cheeseman, G. Scalmani, V. Barone, G. A. Petersson, H. Nakatsuji, X. Li, M. Caricato, A. V. Marenich, J. Bloino, B. G. Janesko, R. Gomperts, B. Mennucci, H. P. Hratchian, J. V. Ortiz, A. F. Izmaylov, J. L. Sonnenberg, D. Williams-Young, F. Ding, F. Lipparini, F. Egidi, J. Goings, B. Peng, A. Petrone, T. Henderson, D. Ranasinghe, V. G. Zakrzewski, J. Gao, N. Rega, G. Zheng, W. Liang, M. Hada, M. Ehara, K. Toyota, R. Fukuda, J. Hasegawa, M. Ishida, T. Nakajima, Y. Honda, O. Kitao, H. Nakai, T. Vreven, K. Throssell, J. A. Montgomery Jr., J. E. Peralta, F. Ogliaro, M. Bearpark, J. J. Heyd, E. N. Brothers, K. N. Kudin, V. N. Staroverov, T. A. Keith, R. Kobayashi, J. Normand, K. Raghavachari, A. P. Rendell, J. C. Burant, S. S. Iyengar, J. Tomasi, M. Cossi, J. M. Millam, M. Klene, C. Adamo, R. Cammi, J. W. Ochterski, R. L. Martin, K. Morokuma, O. Farkas, J. B. Foresman and D. J. Fox, *Gaussian 16, Revision C.01*, Gaussian, Inc., Wallingford CT, 2016.
37 E. I. Sánchez-Flores, R. Chávez-Calvillo, T. A. Keith, G. Cuevas, T. Rocha-Rinza and F. Cortés-Guzmán, *J. Comput. Chem.*, 2014, **35**, 820–828, DOI: **10.1002/jcc.23559**.
38 M. D. Hanwell, D. E. Curtis, D. C. Lonie, T. Vandermeersch, E. Zurek and G. R. Hutchison, *J. Cheminf.*, 2012, **4**, 17.
39 (*a*) J. Pschierer, N. Peschek and H. Plenio, *Green Chem.*, 2010, **12**, 636–642; (*b*) A. Gordillo, E. de Jesus and C. López-Mardomingo, *Chem. Commun.*, 2007, **39**, 4056–4058; (*c*) T. Li, F. Guo, Z. Zha and Z. Wang, *Chem. – Asian J.*, 2013, **8**, 534–537.